A Prediction-Based Link Availability Estimation for Routing Metrics in MANETs

Article *in* IEEE/ACM Transactions on Networking · January 2006

DOI: 10.1109/TNET.2005.860094 · Source: IEEE Xplore

3 authors, including:

Shengming Jiang
Shanghai Maritime University
202 PUBLICATIONS **3,371** CITATIONS
SEE PROFILE

Dajiang he
National University of Singapore
16 PUBLICATIONS **576** CITATIONS
SEE PROFILE

A Prediction-Based Link Availability Estimation for Routing Metrics in MANETs

Shengming Jiang, *Member, IEEE*, Dajiang He, and Jianqiang Rao

***Abstract*—A Mobile Ad hoc Network (MANET) is a collection of wireless mobile terminals that are able to dynamically form a temporary network without any aid from fixed infrastructure or centralized administration. One critical issue for routing in MANETs is how to select reliable paths that can last as long as possible since terminal mobility may cause radio links to be broken frequently. To solve this problem, a criterion that can judge path reliability is needed. The reliability of a path depends on the number of links and the reliability of each link constituting the path. Many routing metrics in terms of number of links have been proposed, such as the shortest path routing. However, how to measure link availability or reliability in order to find more reliable paths has not been addressed adequately in the literature. (By *a link being available*, we mean that the radio quality of the link satisfies the minimum requirement for successful communication. *Link availability* is used to measure probability or degree that a link is available. The terms *availability* and *reliability* are used interchangeable in this paper.) This paper first introduces a prediction-based link availability estimation to quantify the link reliability. This quantity makes use of some instantly available information and also considers the dynamic nature of link status in order to properly reflect the link reliability. Then, this quantity has been further used to develop routing metrics for path selection in terms of path reliability to improve routing performances. The proposed schemes have been investigated through computer simulation.**

***Index Terms*—Link availability, mobile ad hoc networks (MANETs), path reliability, routing metrics, terminal mobility.**

I. Introduction

MANY issues remain to be resolved before Mobile Ad hoc Networks (MANETs) can be efficiently deployed and a number of these issues are related to routing. Routing is difficult in MANETs since terminal mobility may cause radio links to be broken frequently. When any link of a path is broken, this path needs to be either repaired through finding another link or replaced by a newly found path. Such rerouting operation wastes the scarce radio resource and battery power while rerouting delay may affect the quality of service (QoS) and degrade network performance. To reduce rerouting operation, path reliability may be more important in selecting optimal paths in MANETs than other metrics such as path cost and QoS that are often used in wired networks. The reliability of a path depends on the reliability or availability of each link of this path. However, most routing schemes in the literature focus mainly on the procedure of information exchange for finding and/or maintaining a path, and often use *shortest path* (measured in terms of the number of hops or links that a path goes through) as routing metrics [1]. How to measure link availability properly so that it can be used as a routing metric to reflect path reliability has not been addressed adequately.

In [2] and [3], an *associativity* is defined as a new routing metric for link reliability. This metric tries to reflect the degree of the stability of association between two mobile nodes through the connection stability of a node with respect to another one over time and space. Each node generates a beacon to signify its existence periodically. Upon receiving a beacon, the receiver increases the value of its associativity with the beaconing node. In [4], both signal and location stability are used to quantify the reliability of a link. With signal stability, each node classifies its neighbors as either *strongly connected* or *weakly connected* according to the signal strength of received beacons generated periodically by its neighbors. Location stability is measured in terms of the period of time that a link has existed. Accordingly, the routing metric biases the selected path toward the one consisting of strong channels which have been in existence for a time greater than some threshold. A common weakness of the above two pure measurement-based criteria for link reliability is that they cannot reflect possible changes in link status happening in the future. That is, due to the dynamic nature of MANETs, the reliability of a link regarded as *better* based on historical and/or current information on link status may become worse with time than that of those currently measured as *worse*. Such possible misjudgment to link reliability may affect routing performance especially in highly dynamic environments.

A probabilistic link availability model which can predict the future status of a wireless link is proposed in [5] and [6]. In this model, link availability is defined as the probability that there is an active link between two mobile nodes at time t_0+T $(T>0)$ given that this link is available at time t_0. Note that a link will be still considered available at t_0+T even if it experienced failures during one or more intervals between t_0 and t_0+T, and the link availability can be taken as T_a/T, where T_a is the sum of all noncontinuous time periods that the link is available between t_0 and t_0+T. This metric can be used by a node to select more reliable neighbors to form a stabler cluster, but it is impractical for path selection. The reason is if any link of a path fails, rerouting is required immediately, and it is unlikely that related

Manuscript received July 21, 2003; revised November 1, 2004; approved by IEEE/ACM TRANSACTIONS ON NETWORKING Editor N. Shroff. This paper was presented in part at the IEEE INFOCOM, Anchorage, AK, 2001, and the International Workshop on Wireless Networks and Mobile Computing, Taipei, Taiwan, 2000.

S. Jiang is with the School of Electronic and Information Engineering, South China University of Technology, Guangzhou 510640, China. He was with the Institute for Infocomm Research, Singapore 119613 (e-mail: shmjiang@scut.edu.cn).

D. He is with the Networking Department, Institute for Infocomm Research, Singapore 119613 (e-mail: hedj@i2r.a-star.edu.sg).

J. Rao is with Agere Systems, Munich 81669, Germany (e-mail: rao@agere.com).

Digital Object Identifier 10.1109/TNET.2005.860094

nodes will wait for this broken link to become available again. With this consideration, it is more practical to use a continuous time period (T_c) that a link will last from time t_0 to $t_0 + T_c$. However, a longer T_a does not always mean a longer T_c and *vice versa*. Another weakness of this model is that it does not make use of some instant information useful to predict more precisely link availability that can be used to select links in terms of reliability. As shown in [5], this model matches simulation results well when the prediction time periods are longer than tens of minutes. However, it substantially underestimates the link availability for time periods shorter than several minutes, which are actually most interesting to routing since typical flow duration for data applications is often less than several minutes. As an example, the average TCP flow duration is about $12\,\text{s} \sim 19\,\text{s}$ on international Internet links with the U.S. [7].

In this paper, we introduce a prediction-based link availability estimation and routing metrics in terms of path reliability based on this estimation. The basic idea of this estimation is to let a node first predict a continuous time period (T_p) that a currently available link will last its availability from t_0 by assuming that both nodes associated with the link keep their current velocities (i.e., speed and direction) unchanged during T_p. Then, we try to estimate the probability that this link may really last to $t_0 + T_p$, $L(T_p)$, by considering possible changes in velocities occurring between t_0 and $t_0 + T_p$. More precisely, the link availability estimation consists of "unaffected T_p" with the above assumption being held and "affected T_p" with changes in velocities. As discussed later, it is difficult to give an accurate calculation of $L(T_p)$. However, a reasonable estimation of $L(T_p)$ can be still helpful for path selection in terms of reliability. Simulation results have shown that this estimation can reflect the tendency of link availability and can be used to develop path selection metrics to improve network performance. Therefore, pair $[T_p, L(T_p)]$ as a quantity for the link reliability can make use of the instantly available velocities of two nodes of a link with T_p while it also considers the dynamic nature of link status with $L(T_p)$.

The paper is organized as follows. Section II gives a detailed description of the proposed link availability estimation. The results given by this estimation are compared with simulation results in Section III. Some routing metrics in terms of path reliability based on the proposed link availability estimation are discussed in Section IV. Section V summarizes and briefly remarks the paper.

II. Prediction-Based Link Availability Estimation

In this section, we first introduce a measurement-based scheme to predict T_p then focus on $L(T_p)$ estimation. Note that the $L(T_p)$ estimation does not depend on the scheme used to predict T_p provided that T_p is predicted by assuming that no change in velocity happens during T_p.

A. A Measurement-Based T_p Prediction

Assume two mobile nodes *A* and *B* are moving along two solid lines as illustrated in Fig. 1 at speeds of v_a and v_b during an epoch T (an epoch is a random time interval during which a node moves in a constant direction at a constant speed). The

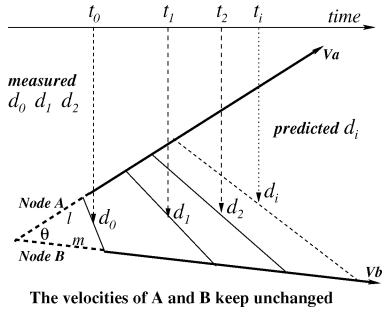

Fig. 1. Schematic for T_p prediction algorithm.

distance d_i between *A* and *B* at $t_i = t_0 + T_i$ can be calculated below according to the triangle theorem. Without loss of generality, let $t_0 = 0$.

$$d_i^2 = (l + v_a T_i)^2 + (m + v_b T_i)^2 - 2\cos\theta (l + v_a T_i)(m + v_b T_i). \quad (1)$$

Since v_a, v_b, l, m, and θ are constant against T_i during T, it is easy to manifest that $\partial^2 d_i^2 / \partial^2 T_i = 0$. So, d_i can be simply expressed as

$$d_i^2 = \alpha T_i^2 + \beta T_i + \gamma \quad (2)$$

where α, β, and γ are constant against T_i. Let d_0, d_1, and d_2 be the distances measured at t_0, t_1, and t_2, respectively. Then, an array of (2) can be formed to sort out α, β, and γ as

$$\begin{cases} \alpha = \dfrac{(d_1^2 t_2 - d_2^2 t_1) - d_0^2 (t_2 - t_1)}{t_1 t_2 (t_1 - t_2)} \\ \beta = \dfrac{(d_1^2 t_2^2 - d_2^2 t_1^2) - d_0^2 (t_2^2 - t_1^2)}{t_1 t_2 (t_2 - t_1)} \\ \gamma = d_0^2. \end{cases} \quad (3)$$

Therefore, d_i at any instant $t_i \le T$ can be calculated by jointly using (2) and (3) based on the measured $d_0 \sim d_2$. Denote $\mathcal{D}$ as the maximum distance between two nodes subject to the minimum radio signal quality for satisfactory communication. Then from (2), we can get (4) to calculate T_p (accounted from t_2) if no change in velocity (i.e., speed and direction) happens.

$$T_p = \frac{\sqrt{\beta^2 + 4\mathcal{D}^2 - 4\alpha\gamma} - \beta}{2\gamma} - t_2. \quad (4)$$

Note that the above calculation does not need knowing v_a, v_b, l, m, and θ although they appear in the derivation. This is important for applicability because it is often very difficult to know these parameters in MANETs.

The accuracy of this T_p prediction depends on the accuracy of the obtained d_i and t_i. If they are accurate, (4) gives an exact T_p prediction. It is relatively easy to get t_i by measuring the time interval between two events. For d_i, one way to estimate it is through measuring received signal strength although in some environments error caused by fading, shadowing or noise may be large. Such methods can be found in many references for cellular radio networks such as [8] and [9]. Recently in [10], a scheme with the similar assumption was proposed to predict T_p based on velocity obtained from Global Position Systems (GPS). This is because, today, multitude of affordable and handheld GPS receivers are available on the market, which may be

used in CDMA-based third-generation cellular systems for the synchronization between base stations and cellular phones [11]. Through GPS, a node can know its position and broadcast this information to its neighbors which can be used to calculate d_i. With this background, we will focus only on $L(T_p)$ estimation by assuming knowing T_p in the following sections.

B. Link Availability Estimation: $L(T_p)$

The basic assumptions for the proposed estimation algorithm are similar to those used in [5] and [6]. That is, 1) terminal mobility is uncorrelated and 2) epochs are exponentially distributed with mean λ^{-1} as

$$A(x) = \mathbb{P}\{\text{epoch} \le x\} = 1 - e^{-\lambda x}. \tag{5}$$

Given a prediction on a continuous available time period $T_p > 0$ for an active link between two nodes at time t_0, the availability of this link, $L(T_p)$, is defined as

$$L(T_p) \triangleq \mathbb{P}\{\text{The availability of a link available at } t_0 \text{will last to } t_0+T_p\} \tag{6}$$

which indicates the probability that the link will be continuously available from time t_0 to $t_0 + T_p$. This definition is used to derive formulas for $L(T_p)$ calculation against T_p. As discussed in Sections II-B.I and III, statistically, $L(T_p)$ can be measured by T_r/T_p, where T_r is the measured time period during which a link predicted to last T_p really lasts.

1) Homogeneous Mean Epoch: To facilitate understanding the proposed estimation, here we first discuss a case that each node has the same mean epoch λ^{-1}. In this case, the calculation of $L(T_p)$ can be divided into two parts: $L_1(T_p)$ if the velocities of the two nodes of the link remain unchanged between t_0 and $t_0 + T_p$, and $L_2(T_p)$ otherwise. That is,

$$L(T_p) = L_1(T_p) + L_2(T_p). \tag{7}$$

It is easy to calculate $L_1(T_p)$, which is just the probability that the epochs from t_0 onwards for the two nodes are longer than T_p. This is because T_p is an accurate prediction when the velocities of the two nodes are unchanged. Since nodes' movements are independent of each other and exponential distribution is "memoryless" [12], $L_1(T_p)$ is given by

$$L_1(T_p) = [1 - A(T_p)]^2 = e^{-2\lambda T_p}. \tag{8}$$

However, it is difficult to give an accurate calculation of $L_2(T_p)$ because of difficulties in learning changes in link status caused by changes in velocity. For example, it is difficult to give a probability for a link to be continuously available after a change in velocity. Nevertheless, in the following, we will discuss an estimation for $L_2(T_p)$.

Denote $\Phi < T_p$ as a random variable for a time interval between t_0 and $t_0 + T_p$ during which either of the two nodes or both change their velocities. $\mathbb{P}\{\phi \le \Phi < T_p\}$ indicates the probability that both nodes keep their velocities unchanged between t_0 and $t_0 + \phi$ while either or both change their velocities after $t_0 + \phi$. The calculation of $\mathbb{P}\{\phi \le \Phi < T_p\}$ also consists of two parts: when only one node changes its velocity and when both nodes change their velocities between $t_0 + \phi$ and $t_0 + T_p$. From the same reason as for deriving (8), $\mathbb{P}\{\phi \le \Phi < T_p\}$ is given by

$$\begin{aligned}\mathbb{P}\{\phi \le \Phi < T_p\} &= 2[A(T_p) - A(\phi)][1 - A(T_p)] + [A(T_p) - A(\phi)]^2 \\ &= e^{-2\lambda\phi} - e^{-2\lambda T_p}.\end{aligned} \tag{9}$$

Then, $\mathcal{L}_2(\phi)$ is introduced to estimate the link availability (as function of ϕ) from $t_0 + \phi$ to $t_0 + T_p$ through calculating the total time (T_t) that the link will be continuously available if changes in velocity happen between t_0 and $t_0 + T_p$. After the first change happens at $t_0 + \phi$, the link is most likely still continuously available if this change makes these two nodes to move close to each other. And this link may be expected to be continuously available most likely from $t_0 + \phi$ to $t_0 + T_p$ if the two nodes keep their velocities unchanged during this period. This happens with probability $e^{-2\lambda(T_p - \phi)}$, which is derived in the same way as for (8). Then, T_t is given by

$$T_t = \phi + (T_p - \phi)pe^{-2\lambda(T_p - \phi)} + \cdots \tag{10}$$

where p is the probability for the two nodes to move close to each other after a change in velocity. Here "..." indicates that an accurate T_t can be achieved by repeating the above calculation for the second possible change during the remaining period and so on as well as the time periods that the link is still continuously available when the two nodes move apart from each other. However, doing so will complicate the calculation. On the other hand, it is reasonable to assume that the contribution of this part to the overall link availability is smaller than the sum of $L_1(T_p)$ and that contributed by the other part on the right-hand side of (10). Therefore, $\epsilon \ge 0$ is introduced to estimate this "..." part. In a more general sense, ϵ tries to include all time periods that are not calculated by the explicit formula but positively contribute to the link availability under estimation. Both p and ϵ are supposed to be independent of ϕ, which will be discussed more later.

So, we can have

$$\mathcal{L}_2(\phi) \triangleq \frac{\phi + (T_p - \phi)pe^{-2\lambda(T_p - \phi)}}{T_p} + \epsilon \tag{11}$$

and $\mathbb{E}[\mathcal{L}_2]$ is used to estimate $L_2(T_p)$, which is defined as

$$\mathbb{E}[\mathcal{L}_2] \triangleq \int_0^{T_p} \mathcal{L}_2(\phi) f(\phi) d\phi \tag{12}$$

where $f(\phi) \ge 0$ is given by

$$\begin{aligned}f(\phi) &= \lim_{\triangle\phi \to 0} \frac{\mathbb{P}\{\phi \le \Phi < T_p\} - \mathbb{P}\{\phi + \triangle\phi \le \Phi < T_p\}}{\triangle\phi} \\ &= -\frac{d\mathbb{P}\{\phi \le \Phi < T_p\}}{d\phi} = 2\lambda e^{-2\lambda\phi}.\end{aligned} \tag{13}$$

Replacing $\mathcal{L}_2(\phi)$ and $f(\phi)$ in (12) with (11) and (13), respectively, we have $\mathbb{E}[\mathcal{L}_2]$ as (note that $\int xe^{ax}dx = e^{ax}(ax-1)/a^2$ [13])

$$\begin{aligned}\mathbb{E}[\mathcal{L}_2] &\approx \int_0^{T_p}\left(\frac{\phi+(T_p-\phi)pe^{-2\lambda(T_p-\phi)}}{T_p}+\epsilon\right)2\lambda e^{-2\lambda\phi}d\phi \\ &= \frac{1}{2\lambda T_p}+\epsilon+e^{-2\lambda T_p}\left(p\lambda T_p-\frac{1}{2\lambda T_p}-\epsilon-1\right). \quad (14)\end{aligned}$$

Then, we have an estimation for $L(T_p)$ as

$$\begin{aligned}L(T_p) &\approx L_1(T_p)+\mathbb{E}[\mathcal{L}_2] \\ &= \frac{1}{2\lambda T_p}+\epsilon+e^{-2\lambda T_p}\left(p\lambda T_p-\frac{1}{2\lambda T_p}-\epsilon\right). \quad (15)\end{aligned}$$

Now we discuss how to determine p and ϵ. Intuitively, in a free environment where there is no border nor predefined movement traces, the two nodes may move either close to or apart away from each other. Since there is no particular factor to affect movements, the above two events should happen in an equal probability such that $p = 0.5$. In this case, (15) can be further simplified into

$$L(T_p) \approx (1-e^{-2\lambda T_p})\left(\frac{1}{2\lambda T_p}+\epsilon\right)+\frac{\lambda T_p e^{-2\lambda T_p}}{2}. \quad (16)$$

Note that this intuitive p setting is not suitable for situations such as indoor environments in which, borders may force nodes to change movement directions back to the space. This may cause event "moving close" to happen more frequently than "moving apart away." However, it is difficult to mathematically determine p for various environments. For simplicity, we suggest to use $p = 0.5$ and adjust the discrepancy of link availability through measuring ϵ as discussed below.

The value of ϵ mainly depends on environmental factors such as node density, radio coverage and space sizes. Since these factors change with time and movement, it is impossible to have a formula for ϵ that can adapt for these changes. With this respect, it is more practical to devise a measurement for ϵ, which can also make the proposed estimation adaptive to environmental changes. That is, after a node has a prediction T_p on a link at time t_0, it then measures the duration (T_r) that this link will really last from t_0. If this link is still available after t_0+T_p, it does another prediction. Thus, a measured $L(T_p)$ for T_p, $L_m(T_p)$, is given by T_r/T_p. If multiple $T_{r,i}$ $(i = 1 \ldots N_{T_r})$ are collected for one T_p, the final $L_m(T_p)$ for this T_p is given by $(1/N_{T_r})\sum_{i=1}^{N_{T_r}}(T_{r,i}/T_p)$. Replacing $L(T_p)$ in (16) with $L_m(T_p)$, we have a measured ϵ corresponding to this T_p as

$$\epsilon_m \approx \frac{L_m(T_p)-\frac{1}{2}\lambda T_p e^{-2\lambda T_p}}{1-e^{-2\lambda T_p}}-\frac{1}{2\lambda T_p}. \quad (17)$$

Repeating the above operation for different T_p, $T_{p,j}$ $(j = 1 \ldots N_{T_p})$, we can have a series of ϵ_m, $\epsilon_{m,j}$. Then, ϵ can be estimated by $(1/N_{T_p})\sum_{j=1}^{N_{T_p}}\epsilon_{m,j}$. Note that individual ϵ_m for some $L_m(T_p)$ may be negative due to the dynamic nature of link status but not for the averaged ϵ_m over sufficient samples according to its definition.

At the beginning of the operation, a node can set $\epsilon = 0$, with which (16) gives a conservative link availability estimation, $L_{\min}(T_p)$, as

$$L_{\min}(T_p) = \frac{1-e^{-2\lambda T_p}}{2\lambda T_p}+\frac{\lambda T_p e^{-2\lambda T_p}}{2}. \quad (18)$$

From the above discussion, we can find that a simple and accurate calculation of $L(T_p)$ is not easy even for the mobility model with the exponential distribution (for epochs) which is well known for simple modeling. The simplicity of $L(T_p)$ calculation is important since this calculation is performed "on-the-fly" for routing decision and because of the power limitation of nodes in MANETs. Therefore, a challenging issue is how to have such a $L(T_p)$ calculation for all possible mobility models since mobile nodes often roam. However, it is difficult to address this issue completely since we do not know a model that can describe all possible mobile behaviors. The method discussed above outlines a framework of possible solutions to this issue, i.e., having an estimation based on one typical mobility model first and then using measurement to adjust discrepancy with other models. More works are required to find the typical mobility model that can best describe all possible mobile behaviors.

2) Heterogeneous Mean Epochs: Here we extend the above derivation to the case of different mean epochs for the two nodes of a link, i.e.,

$$A_1(x) = 1-e^{-\lambda_1 x} \text{ and } A_2(x) = 1-e^{-\lambda_2 x}.$$

In the same way as for the homogeneous case, we can have $L_1(T_p)$ as

$$L_1(T_p) = [1-A_1(T_p)][1-A_2(T_p)] = e^{-(\lambda_1+\lambda_2)T_p}. \quad (19)$$

Similarly,

$$\mathcal{L}_2(\phi) = \frac{\phi+(T_p-\phi)pe^{-(\lambda_1+\lambda_2)(T_p-\phi)}}{T_p}+\epsilon. \quad (20)$$

Since

$$\begin{aligned}\mathbb{P}\{\phi \le \Phi < T_p\} &= [A_1(T_p)-A_1(\phi)][1-A_2(T_p)] \\ &\quad +[A_2(T_p)-A_2(\phi)][1-A_1(T_p)] \\ &\quad +[A_1(T_p)-A_1(\phi)][A_2(T_p)-A_2(\phi)] \\ &= e^{-(\lambda_1+\lambda_2)\phi}-e^{-(\lambda_1+\lambda_2)T_p} \quad (21)\end{aligned}$$

we have $f(\phi) = (\lambda_1+\lambda_2)e^{-(\lambda_1+\lambda_2)\phi}$. Therefore,

$$\begin{aligned}\mathbb{E}[\mathcal{L}_2] &= \int_0^{T_p}\mathcal{L}_2(\phi)f(\phi)d\phi \\ &= \frac{e^{-(\lambda_1+\lambda_2)T_p}}{\lambda_1+\lambda_2}\left\{\frac{pT_p}{2}(\lambda_1^2+\lambda_2^2)-\lambda_2(1+\epsilon)\right. \\ &\quad +e^{(\lambda_1+\lambda_2)T_p}\left[\frac{1}{T_p}+(\lambda_1+\lambda_2)\epsilon\right] \\ &\quad \left.-\lambda_1(1+\epsilon-pT_p\lambda_2)-\frac{1}{T_p}\right\}. \quad (22)\end{aligned}$$

Summing (19) and (22), we have $L(T_p)$ as

$$L(T_p) \approx \frac{e^{-(\lambda_1+\lambda_2)T_p}}{\lambda_1+\lambda_2}\left\{\frac{pT_p}{2}(\lambda_1+\lambda_2)^2-(\lambda_1+\lambda_2)\epsilon-\frac{1}{T_p} +e^{(\lambda_1+\lambda_2)T_p}\left[\frac{1}{T_p}+(\lambda_1+\lambda_2)\epsilon\right]\right\}. \quad (23)$$

Letting $\lambda_1=\lambda_2=\lambda$ in (23), we can have (15).

Similarly, letting $\epsilon=0$, we have

$$L_{\min}(T_p)=\frac{e^{-(\lambda_1+\lambda_2)T_p}}{(\lambda_1+\lambda_2)T_p}\left[\frac{p}{2}T_p^2(\lambda_1+\lambda_2)^2+e^{(\lambda_1+\lambda_2)T_p}-1\right]. \quad (24)$$

The above estimation of $L(T_p)$ is useful in an integrated environment such as a cellular network integrated with an MANET [14], where some low mobility or stationary nodes can sever as routers. In this case, the mean epoch of such nodes, say λ_2^{-1}, is very large or infinity. If $\lambda_2^{-1}=\infty$, (23) and (24) can be further simplified into

$$L(T_p) \approx e^{-\lambda_1 T_p}\left[\frac{pT_p\lambda_1}{2}-\frac{1}{T_p\lambda_1}-\epsilon+e^{\lambda_1 T_p}\left(\frac{1}{T_p\lambda_1}+\epsilon\right)\right] \quad (25)$$

and

$$L_{\min}(T_p)=\frac{e^{-\lambda_1 T_p}}{\lambda_1 T_p}\left[\frac{p}{2}T_p^2\lambda_1^2+e^{\lambda_1 T_p}-1\right]. \quad (26)$$

The values of p and ϵ can be obtained in the same way as for the homogeneous case discussed in Section II-B.1. To let a node learn λ of other nodes, λ needs to be broadcast through either beacon messages or piggyback mechanism by amending some existing protocols. For example, for DSR, λ can be embedded into the Route Request packet.

III. Numerical Results

Since the above section only provides an estimation of $L(T_p)$ other than its exact calculation, it is important to investigate the accuracy of the proposed estimation. Here, we verify the estimation for the homogeneous case through computer simulation in OPNET [15]. The environment under simulation is a two-dimensional space, in which there are 30 nodes moving randomly according to given mobility models. The maximum radius of a mobile's radio coverage $\mathcal{D}$ is 300 m, which is a design parameter of some typical IEEE 802.11 products such as [16]. A node's transmission rate is 2 Mb/s and IEEE 802.11 is adopted for the MAC layer. Mobility models with both exponentially and non-exponentially distributed epochs are investigated. The method introduced in Section II-A is used to predict T_p.

The simulation results are plotted with the x-axis being converged T_p and the y-axis being converged $L_m(T_p)$ because too many points have been collected from the simulation. The convergence is done as follows: if there are J triplets $\langle T_{p,j}, L_m(T_{p,j}), N_j\rangle$, in which $I \le T_{p,j} < I+1$ (I is an integer and $j=1\ldots J$), where N_j is the times of $T_{p,j}$ occurrence. This series is converged into one point as

$$x=\frac{\sum_{j=1}^{J} T_{p,j}N_j}{\sum_{j=1}^{J} N_j} \text{ and } y=\frac{\sum_{j=1}^{J} L_m(T_{p,j})N_j}{\sum_{j=1}^{J} N_j}.$$

Then, x and y are used to replace T_p and $L_m(T_p)$, respectively, in (17) to calculate ϵ_m, and the final ϵ is calculated over all converged points. This ϵ is used by (16) to plot $L(T_p)$. Since the value of predicted T_p ranges from 0 to hundreds, even thousands, of seconds (which mainly depends on λ^{-1}), the above convergence can show the tendency of simulation results more clearly without losing accuracy.

We first look at the results for the random-walk-based mobility model [6]. With this model, a node selects a direction uniformly from a given space and a speed uniformly from 0 to 20 m/s for its next movement. The epoch of the above movement is selected according to an exponential distribution with mean λ^{-1}. This model allows a node to move beyond the allowed space. But the direction of its next movement following "moving out" is forced to the space in order to maintain node density in the simulation.

Fig. 2(a) plots simulation results in dotted lines (i.e., "Sim" in the figure) and estimated results (i.e., "Est" in the figure) given by (16) in a solid line for space $(500\text{ m})^2$ and $\lambda^{-1}=60$ s. We can find that simulation results fluctuate almost around the curve given by $L(T_p)$. This indicates that $L(T_p)$ can approximate $\overline{T}_r/T_p$ in this case, where $\overline{T}_r$ is the mean time period that a link will be continuously available corresponding to a predicted T_p. However, there is a substantial mismatch between them when T_p is very short since a "quasi-bell shape" appears in simulation results but not in estimated results. Intuitively, the shorter T_p, the higher $L(T_p)$ should be. We think that this phenomenon is mainly caused by a poor simulation of the memoryless property of exponential distribution, as explained below.

As illustrated in Fig. 3, in the simulation, a node randomly generates an epoch (e) and a velocity (v) for its next movement at time t. To save simulation time and simplify simulation, the above operation will be only repeated at $t+e$ and so on. Thus, the generated e will remain unchanged until $t+e$. On the other hand, T_p prediction is independent of the above e generation. Assume a T_p is predicted at time t_0 ($t<t_0\le t+e$). As illustrated in Fig. 3, t_0+T_p may be either later (case i) or earlier (case ii, including "equal to") than $t+e$. In case i, the epoch will be regenerated randomly at $t+e$. However, in case ii, the epoch is no longer random to T_p relatively. This factor affects the accuracy of the above link availability estimation based on the memoryless property which ensures that epoch from t_0 onwards will follow the same distribution as $A(x)$ with the same λ^{-1}.

It seems possible to remedy the above loss of the memoryless property by letting a node randomly regenerate epochs in case ii at t_0. However, doing so violates another assumption on the independence of node movements since it may force the related nodes to change their epochs at the same time. Here, we do not discuss a fully amended formula for (15) subject to the above

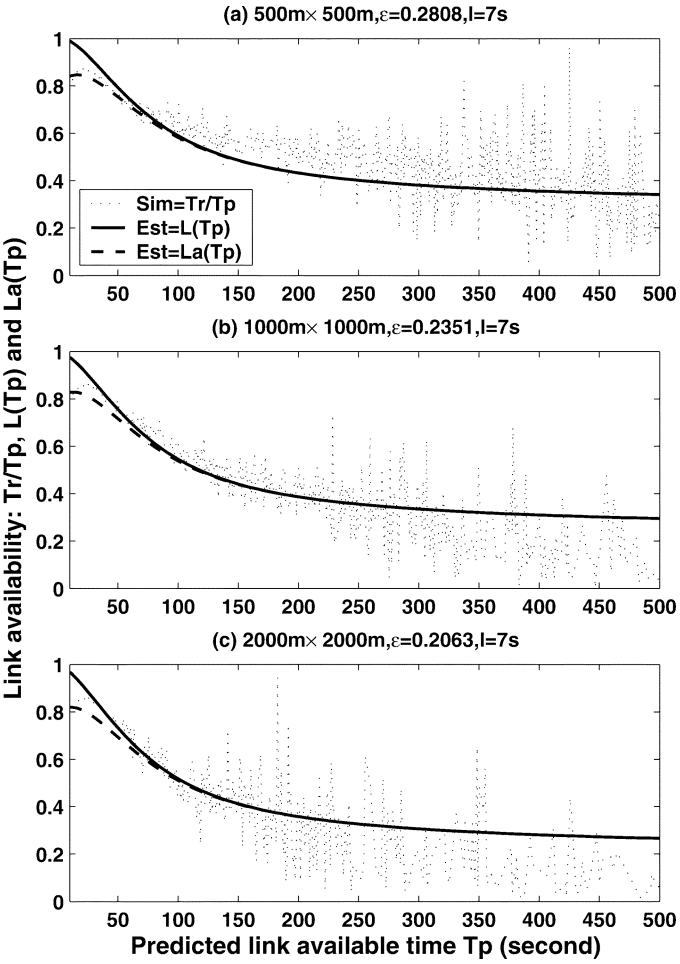

Fig. 2. Random-walk-based model: $\lambda^{-1} = 60$ s.

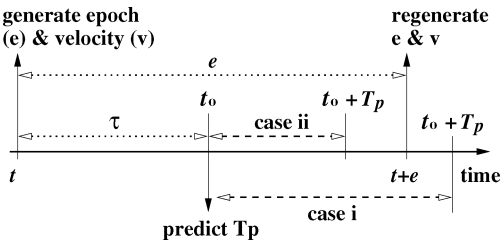

Fig. 3. Simulation model for epoch generation and T_p prediction.

mentioned factor since it will not happen in real environments. Nevertheless, to verify the above analysis, a simple amendment to (15) is discussed below.

It is easier to amend $L_1(T_p)$ than $L_2(T_p)$ with the same reason as for calculating $L_2(T_p)$ discussed earlier. So, we only discuss an amended $L_1(T_p)$ here. As mentioned earlier, $L_1(T_p)$ is the probability for both nodes to keep their velocities unchanged between t_0 and $t_0 + T_p$. With the memoryless property, $L_1(T_p) = [1 - A(T_p)]^2$ since there is no need to consider what happens before t_0 so that the epoch can be counted from t_0 in this case. However, due to the lack of the memoryless property caused by the simulation as illustrated in Fig. 3, the epoch should be counted from t at which the last change in velocity happens rather than from t_0. So, no change happening during the period from t_0 to $t_0 + T_p$ is equivalent to that from t to $t_0 + T_p$ since the simulation guarantees no change to happen during the period from t to t_0. The probability for the former event to happen in one node is $1 - A(\tau + T_p)$, where τ is the offset between t and t_0 as illustrated in the figure. There are two nodes associated with a link and t for one node may be different from that of the other. So in this case, $L_1(T_p)$ should be estimated by $[1 - A(l + T_p)]^2$, where l is the averaged τ. Therefore, an amended (15), $L_a(T_p)$, is approximated by

$$L_a(T_p) \approx e^{-2\lambda(l+T_p)} + \frac{1}{2\lambda T_p} + \epsilon + e^{-2\lambda T_p}\left(p\lambda T_p - \frac{1}{2\lambda T_p} - \epsilon - 1\right). \quad (27)$$

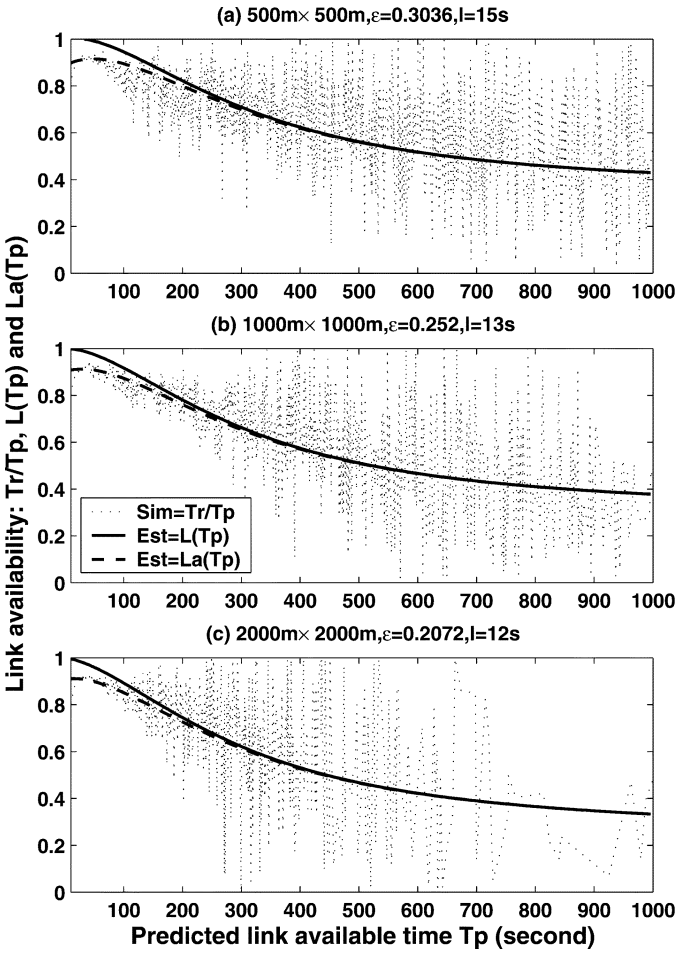

Fig. 4. Random-walk-based model: $\lambda^{-1} = 250$ s.

The dashed line in Fig. 2(a) is plotted according to (27) with $p = 0.5$ and an experimental $l = 7$ s which is obtained by matching estimated results with simulation results. This curve shows a tendency similar to simulation results. Since case ii happens relatively frequently for small T_p (compared to λ^{-1}), this mismatch mainly appears in small T_p region. To reduce inaccuracy to measured ϵ caused by this mismatch, we avoid measuring ϵ for very short T_p. Here, measuring ϵ roughly starts from $T_p \geq 0.5\lambda^{-1}$.

Fig. 2(b)–(c) show results for spaces $(1000\ \text{m})^2$ and $(2000\ \text{m})^2$, which both give lower node density than $(500\ \text{m})^2$. It can be found that estimated results are a

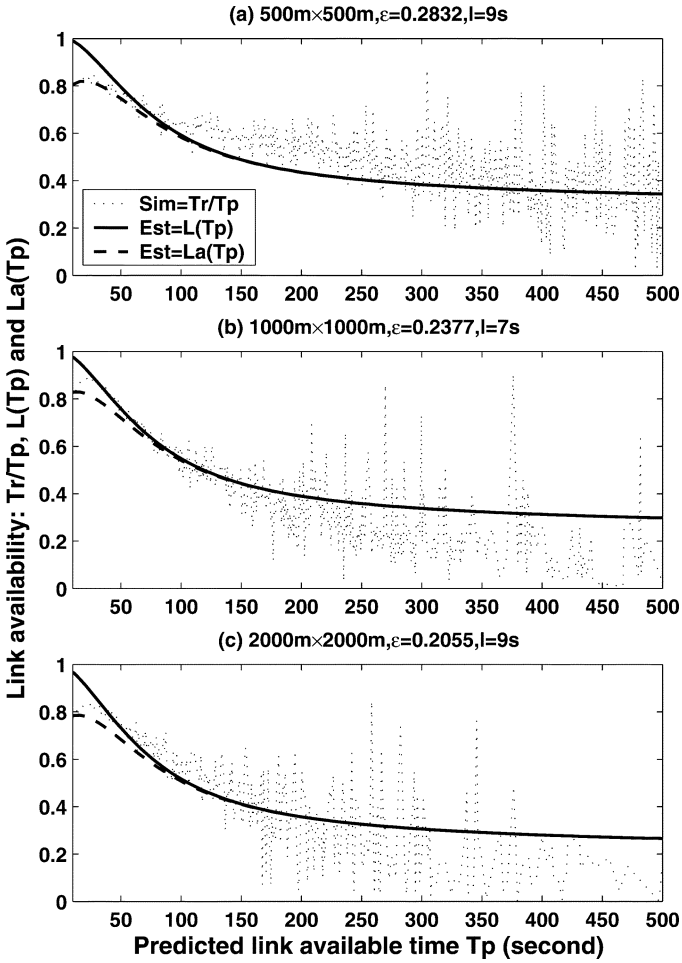

Fig. 5. Exponential random way point model: $\lambda^{-1} = 60$ s.

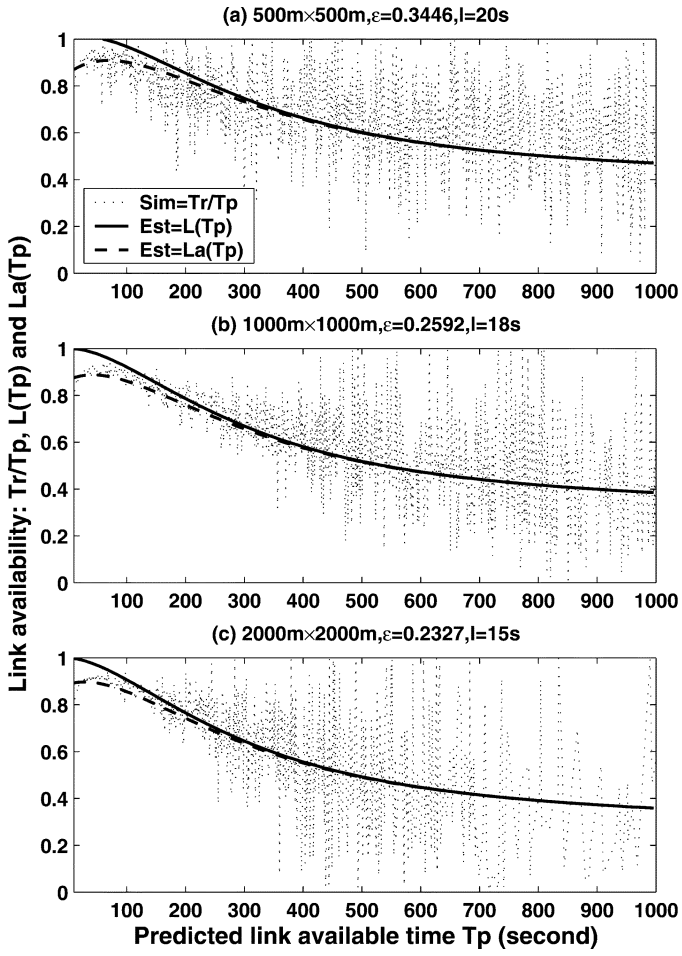

Fig. 6. Exponential random way point model: $\lambda^{-1} = 250$ s.

little higher than simulation results (on average) when T_p is large. This is because the number of events for large T_p is much less than that for small T_p with short λ^{-1} as shown in the figures. Let x denote epoch. For example, $\mathbb{P}\{x > 350|\lambda^{-1} = 60\} = 1 - A(350) = 0.0029$ while $\mathbb{P}\{200 \geq x > 100|\lambda^{-1} = 60\} = A(200) - A(100) = 0.1532$. As mentioned earlier, ϵ used in the estimation is measured over simulation results. It is true for most measurement that the final result tends to reflect frequently occurring events. Therefore, the above phenomenon almost disappears in simulations with long λ^{-1} as shown in Fig. 4, in which more events for large T_p values are generated with large $\lambda^{-1} = 250$ s. In this case, $\mathbb{P}\{x > 700|\lambda^{-1} = 250\} = 0.061 \gg 0.0029$.

It can also be found that results estimated by $L(T_p)$ in Fig. 4(a) tends to go beyond 1 when T_p is small. This is because the final measured ϵ has not taken into account the results for small T_p as mentioned earlier. When λ^{-1} becomes longer, case ii mentioned above will happen more frequently and causes a larger mismatch between simulation results and results estimated by $L(T_p)$. $L_a(T_p)$ almost amends this problem as shown in this figure. Despite the above case for small T_p, we can find that, the estimated results can generally reflect the tendency of the simulation results.

From ϵ listed in the titles of Figs. 2–4, we can find that it generally decreases as space sizes increase for one λ^{-1}. This indicates that probability for an available link between a pair of nodes to keep available after a change in their velocities becomes small as node density decreases. Therefore, in the case of uncertainty about ϵ, it is conservative to set $\epsilon = 0$, i.e., using $L_{\min}(T_p)$ given by (18).

Now we look at results for the exponential random way point model. In this model, a node selects uniformly a random destination point within a given space. The time for this node to reach the destination (i.e., epoch) is selected according to an exponential distribution with mean λ^{-1}. Its speed is just the ratio of the distance between its current position and the selected destination to the epoch. Upon reaching the destination, the node repeats the above operation. During its movement to the destination, its velocity keeps unchanged. This model is different from the random-walk-based model in terms of: 1) a node can move only within the allowed space and 2) its speed is nonuniformly distributed without a predefined limit.

As shown in Fig. 5 for $\lambda^{-1} = 60$ s, the phenomena here are similar to those in the random-walk-based model for respective space sizes and so is for ϵ as listed therein. Fig. 6[1] for $\lambda^{-1} = 250$ s show that the estimated results match well the simulation results. However, in terms of ϵ for $\lambda^{-1} = 250$ s,

[1]The figure here corrects errors in the estimation results in Figs. 8–9 (dashed lines) of our INFOCOM'01 paper for spaces $(500\text{ m})^2$ and $(1000\text{ m})^2$. These errors are due to misusing $\lambda^{-1} = 60$ s for $\lambda^{-1} = 250$ s in the estimation.

there is a big difference between these two mobility models. As mentioned earlier, a larger ϵ indicates a larger probability for an active link to be continuously available after changes in velocity. This means that this probability with the exponential random way point model is larger than that with the random-walk-based model. This is because the random-walk-based model allows nodes to move beyond the allowed space, resulting in lower node density compared with the exponential random way point model. Furthermore, the time for a node to stay outside of the space is proportional to its epoch which depends on λ^{-1}. This can explain why the above difference is not so obvious for $\lambda^{-1} = 60$ s.

Note that the fluctuation of measured T_r/T_p is significant as shown in the above figures. These fluctuations somewhat reflect the nature of link reliability and it is difficult to theoretically match them. Therefore, the calculated $L(T_p)$ does not actually reflect the reliability of a link instantly but statistically to capture the curve that measured T_r/T_p fluctuates around.

At last, we check the possible applicability of the proposed link availability estimation for a model with nonexponentially distributed epochs, the random way point model [17]. The only difference from the above exponential random way point model is that here speed is selected uniformly from 0 to 20 *m/s* while the epoch is the ratio of the distance to the speed. In this case, it is difficult to quantify the epoch distribution and λ^{-1}. Here, we obtain λ^{-1} through statistics on simulation results. As shown in Fig. 7, it is not strange that the estimation for this model is not so good as that for the exponential models discussed above. However, it is interesting that the mismatch between the estimation and the simulation becomes smaller as space size increases. This is probably because the intuitive setting $p = 0.5$ is suitable for spacious space as mentioned in Section II-B.I. We can also find that the minimal link availability $L_{\min}(T_p)$ given by (18) in circled lines can be still suitable for this case (on average) as shown in these figures. However, to have better $L(T_p)$ estimation for nonexponentially distributed epochs, more studies are still needed.

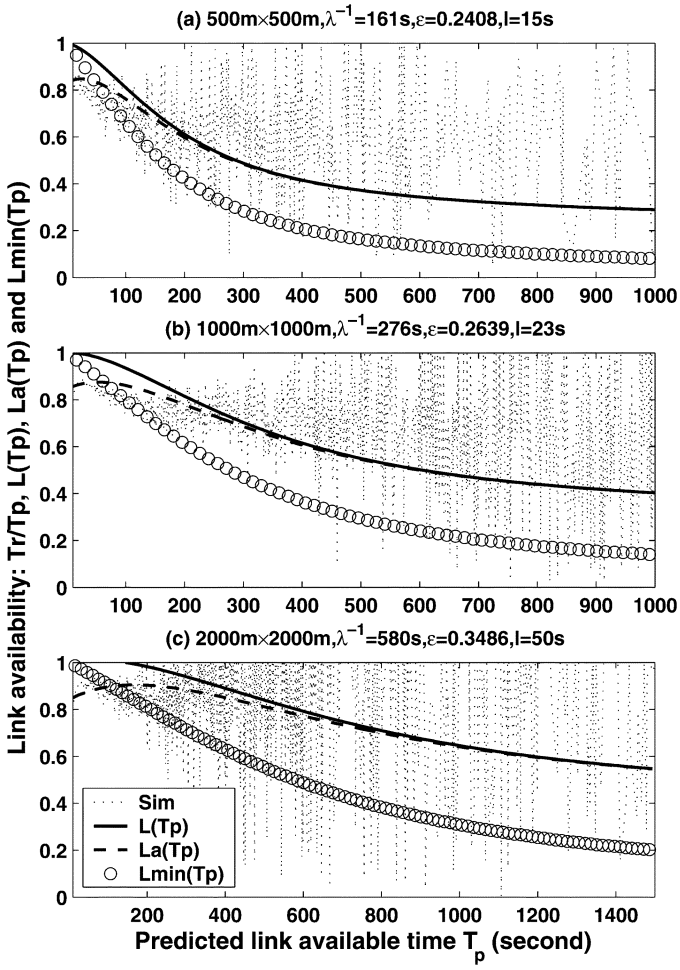

Fig. 7. Random way point model (nonexponential distributed epochs).

IV. Routing Metrics Based on $T_p \times L(T_p)$

One practical interest of the proposed estimation is to develop a path selection metric in terms of path reliability because T_p alone cannot properly judge link availability. For example, given two links: **L1** with $T_p = 10$ s and $L(T_p) = 0.001$ while **L2** with $T_p = 5$ s and $L(T_p) = 0.1$, only using T_p as the metric, we will select **L1**. But its mean available time $10 \times 0.001 = 0.01$ s is much smaller than $5 \times 0.1 = 0.5$ s of **L2**. Therefore, it is better to use $T_p \times L(T_p)$ as the link reliability metric.

For a path consisting of multiple links, its reliability mainly depends on the weakest link in terms of reliability that can be measured by $\overline{T}_r \approx T_p \times L(T_p)$. A link with a smallest $\overline{T}_r$, i.e., $\overline{T}_{\min}$, is considered as the weakest link. An ideal path in terms of path reliability should be the one with the maximum $\overline{T}_{\min}$ and the minimum number of links. In the following, we show through computer simulation some performance differences given by the Dynamic Source Routing (DSR) protocol [18] using the above routing metric and classical routing metrics which are described below. The same simulation model as used in Section III is adopted here. A source node transmits data packets at fixed packet rates, and packet length is also fixed at 64 bytes.

The following routing metrics are adopted in the simulation.

- *First Found Path* (FFP): The first found path is selected. For example, in DSR, the path carried by the first routing reply packet received by the source node is selected.
- *Shortest Path* (SP): The path going through the minimum number of hops is selected.
- *Shortest Path with* $\overline{T}_r$ (SPL): This is what have been discussed above. According to link availability estimation formulas, this metric can be further classified as follows:

1. SPL_o: $\overline{T}_r \approx T_p \times L(T_p)$ with (16);
2. SPL_m: $\overline{T}_r \approx T_p \times L_{\min}(T_p)$ with (18);
3. SPL_a: $\overline{T}_r \approx T_p \times L_a(T_p)$ with (27).

The performances of routing metrics are measured in terms of:

- *packet loss ratio*: the number of lost data packets to the number of transmitted data packets;
- *end-to-end delay* (second): the average delay experienced by the received user packets;
- *goodput* (packets/s): the number of received data packets over simulation time, which can be estimated by (1 − packet loss ratio) × (packet transmission rate).

TABLE I
COMPARISON FOR RANDOM WALK-BASED MODEL: $(500\ \mathrm{m})^2$, 5 FLOWS, $\lambda^{-1} = 60$ s

	loss	delay	goodput	Δ_1	Δ_2
FFP	0.6613	45.03	16.94	-	-
SP	0.7104	24.29	14.48	-	-
SPL_o	0.6346	13.79	18.27	7.9	26.2
SPL_m	0.6346	13.79	18.27	7.9	26.2
SPL_a	0.6346	13.79	18.27	7.9	26.2
FFP	0.8562	3.51	14.38	-	-
SP	0.87	19.99	13	-	-
SPL_o	0.6626	27.19	33.74	134.6	159.5
SPL_m	0.6564	30.21	34.36	138.9	164.3
SPL_a	0.6564	30.21	34.36	138.9	164.3

-Upper half for transmission rate of '10 packets/s/flow';
-Lower half for '20 packets/s/flow'.

For comparison, goodput improvement ratio (Δ) is also defined, which is the ratio of the goodput given by SPL_x (denoted by G) to that given by another routing metric such as FFP and SP (denoted by g) minus 1, i.e., $\Delta = G/g - 1$.

Table I lists simulation results for the random-walk-based model with two packet transmission rates. We can find that SPL_x ($x = o, m,$ or a) is the best in terms of goodput. Since the delay is measured only for received packets, it becomes shorter when packet loss ratio reaches some values. This is because DSR drops the buffered packets that have been queued for certain threshold (here 30 s). When a path is down, rerouting may contribute significantly to queueing delay, resulting in more long-delayed packets to be dropped. This phenomenon becomes more obvious for heavy load as shown in this table.

Columns Δ_1 and Δ_2 show the goodput improvement ratios given by SPL_x over FFP and SP, respectively. We can find that this improvement increases with traffic load. However, there is almost no difference in performances between SPL_x, especially in the case of 10 packets/s. This is because, although the three metrics give different values of $\overline{T}_r$, they are almost similar in reflecting the relative degree of path reliability so that they may select the same path. This can be somewhat further shown below.

Given an environment, ϵ can be treated as a constant against T_p. So, SPL_o and SPL_m can be further simplified into just judging T_p instead of $\overline{T}_r = T_p \times L(T_p)$ to avoid calculating $L(T_p)$ every time. We can get $\partial\overline{T}_r/\partial T_p$ from (16) as

$$\frac{\partial \overline{T}_r}{\partial T_p} = e^{-2\lambda T_p}(1 + \lambda T_p - \lambda^2 {T_p}^2) \tag{28}$$

for both SPL_o and SPL_m. It is easy to get a T_p, $\hat{T}_p$, corresponding to the peak of $\overline{T}_r$ against T_p by taking $\partial\overline{T}_r/\partial T_p = 0$, as

$$\hat{T}_p = \frac{1+\sqrt{5}}{2}\lambda^{-1} \approx 1.618\lambda^{-1}. \tag{29}$$

It is also easy to show that $\overline{T}_r$ increases with T_p if $T_p \le \hat{T}_p$ and decreases otherwise. Therefore, an ideal link in terms of reliability should be one with the maximum T_p if $T_p \le \hat{T}_p$ while with the minimum T_p otherwise. However, when there are some T_p smaller than $\hat{T}_p$ while some larger than $\hat{T}_p$, $\overline{T}_r$ is still required to judge the reliability.

TABLE II
COMPARISON BETWEEN RWP AND ERWP: $(1000\ \mathrm{m})^2$, 5 FLOWS, 10 PACKETS/S/FLOW

models	metric	loss	delay	goodput	Δ
eRWP/w	SP	0.6009	1.379	19.96	-
λ^{-1}=60s	SPL_m	0.5954	4.039	20.23	1.4
RWP/w	SP	0.0601	0.03	46.99	-
λ^{-1}=276s	SPL_m	0.0634	0.04	46.83	-0.3
RWP/w	SP	0.0357	0.096	48.22	-
λ^{-1}=56s	SPL_m	0.0296	0.162	48.5	0.6

RWP (eRWP) = (exponential) random way point model.

TABLE III
COMPARISON BETWEEN SPL_o AND SPL_o^+: $(500\ \mathrm{m})^2$, 10 FLOWS, 10 PACKETS/S/FLOW, $\lambda^{-1} = 60$ s

	Random-way point				Random-walk			
	loss	delay	GP	Δ	loss	delay	GP	Δ
SP	0.107	0.021	89.3	-	0.835	2.02	16.5	-
SPL_o	0.1	0.025	90	0.8	0.822	3.29	17.8	7.9
SPL_o^+	0.09	0.027	91	1.9	0.809	1.13	19.1	15.8

GP stands for 'goodput'.

Table II lists results of SP and SPL_m for the original and the exponential random way point models (RWP/eRWP). Here, column Δ shows the goodput improvement ratio given by SPL_m over SP. We can find that differences in goodput are very small. This is because mobility is almost not a major concern for routing in terms of path reliability in this case. As mentioned in Section III, the random way point model has a higher connectivity than the random-walk-based model since the latter allows nodes to move beyond the space. Consequently, probabilities for a path to be broken due to mobility are low in this case. Furthermore, $\lambda^{-1} = 276$ s used in the original model indicates that frequency for a node to change its velocity is much low. This further dilutes the effect of mobility on performance. We can also find a small improvement for $\lambda^{-1} = 56$ s despite the nonexponentially distributed epoch.

Although the above proposed routing metrics can reduce rerouting frequency, rerouting may still happen. Here, we further introduce a joint use of the above routing metrics and a proactive rerouting approach for better performance improvement. Generally, the accuracy of the T_p prediction is high for short T_p. Once such a T_p (here 2 s) is predicted for an active path, it is more likely that this path will be down soon. Instead of rerouting after the path is effectively down, we suggest to trigger a rerouting immediately to find a new path before the old one is down. By doing so, it is believed that the disruption of packet flow caused by mobility can be decreased. Table III compares results given by SP, SPL_o and SPL_o plus the proposed proactive rerouting (SPL_o^+). As shown by column Δ in the table, with the less mobility sensitive random way point model, the difference between SPL_o and SPL_o^+ is small. However, the goodput improvement by SPL_o^+ over SP is about twice of that given by SPL_o alone with the more mobility sensitive random-walk-based model.

Here we do not try to claim that SPL_x is the best routing metric. What has been shown here is that routing performance (e.g., goodput) can be further improved with a proper consideration of path reliability when mobility is a major concern in

routing. By "proper," we mean that some method to judge path reliability is necessary. The proposed link availability estimation along with routing metrics is just such an effort. We have investigated this effort by combining the link availability estimation with the popular SP routing metric. In general, the reliability of a path is reversely proportional to the number of hops or links it goes through. Therefore, SP is better than other routing metrics in terms of path reliability. The performance improvement shown here indicates that the proposed link availability estimation can help SP in selecting more reliable paths.

V. Summary and Remarks

In this paper, we have proposed: 1) quantity $[T_p, L(T_p)]$ for the link availability, which exploits instantly available velocity to predict T_p and reflects the dynamic nature of link status with $L(T_p)$; 2) a method to predict T_p; and 3) an estimation of $L(T_p)$. Particularly, we focused on 3) since T_p may also be predicted with other methods such as using GPS. A simulation study has been conducted to validate the proposed $L(T_p)$ estimation, which shows that the estimation can reflect the general tendency of link availability statistically. That is, $L(T_p)$ can approximate $\overline{T}_r/T_p$, where $\overline{T}_r$ is the mean time that a link will be continuously available during period T_p. We have also briefly investigated an application of $[T_p, L(T_p)]$ in DSR for routing metrics based on the proposed $L(T_p)$ estimation. Simulation results have shown that when $T_p \times L(T_p)$ is adopted in path selection as a reliability metric, performance can be improved significantly in mobility-sensitive environments, and further improvement can be achieved in couple with the proactive rerouting approach introduced in this paper.

The proposed T_p estimation is based on a mobility model with exponentially distributed epochs for simple analysis. Both intuitive setting and measurement are used jointly to determine p and ϵ, respectively. Since it is very difficult to use one mobility model to describe all mobile behaviors when mobile nodes roam across different environments, we also expect that the measured ϵ can provide the proposed $L(T_p)$ estimation with certain adaptability to other mobility models. However, more effort is still needed to make the estimation better since the results for the nonexponential model are not so good as for the exponential model under investigation. This may be achieved by finding a mobility-adaptive measurement for p to replace the intuitive setting. It is also possible to find a nonexponentially distributed epoch model which is better than the exponential one to describe various mobile behaviors. Last but not least, detailed investigations on the effect of using the proposed quantity to applications and a study on implementing the proposal in real MANETs are necessary. Our recent paper [19] reports a follow-up work on how to use this method to estimate link caching time and to select a lower mobility nodes as next hops in order to improve DSR's performance.

Acknowledgment

The authors would like to thank the anonymous reviewers for their valuable comments and the editors for their time spent in handling the paper.

References

[1] E. M. Royer and C. K. Toh, "A review of current routing protocols for ad hoc mobile wireless networks," *IEEE Pers. Commun. Mag.*, no. 2, pp. 46–55, Apr. 1999.
[2] C. K. Toh, "Associativity-based routing for ad hoc networks," *Wireless Pers. Commun.*, vol. 4, no. 2, pp. 103–139, Mar. 1997.
[3] ——, *Wireless ATM and Ad-Hoc Networks*. Boston, MA: Kluwer Academic, 1996.
[4] R. Dube, C. Raia, K.-Y. Wang, and S. Tripathi, "Signal stability based adaptive routing (SSA) for ad hoc networks," *IEEE Pers. Commun. Mag.*, no. 2, pp. 36–45, Feb. 1997.
[5] A. B. McDonald and T. F. Znabi, "A path availability model for wireless ad hoc networks," in *Proc. IEEE WCNC*, New Orlean, LA, Sep. 1999, pp. 35–40.
[6] ——, "A mobility-based framework for adaptive clustering in wireless ad hoc networks," *IEEE J. Sel. Areas Commun.*, vol. 17, no. 8, pp. 1466–1487, Aug. 1999.
[7] K. Thompson, G. J. Miler, and R. Wilder, "Wide-area internet traffic patterns and characteristics," *IEEE Network Mag.*, vol. 11, no. 6, pp. 10–23, Nov./Dec. 1997.
[8] M. Hellebrandt, R. Mathar, and M. Scheibenbogen, "Estimating position and velocity of mobiles in a cellular radio network," *IEEE Trans. Veh. Technol.*, vol. 46, no. 1, pp. 65–71, Feb. 1997.
[9] T. Liu, P. Bahl, and I. Chlamtac, "An optimal self-learning estimator for predicting inter-cell user trajectory in wireless radio networks," in *Proc. IEEE ICUPC*, San Diego, CA, Oct. 1997, pp. 438–442.
[10] W. Su and M. Gerla, "IPv6 flow handoff in ad hoc wireless networks using mobility predication," in *Proc. IEEE GLOBECOM*, Rio De Janeiro, Brazil, Dec. 1999, pp. 271–275.
[11] E. A. Bretz and T. S. Perry, "X marks the spot, maybe," *IEEE Spectrum*, vol. 37, no. 4, pp. 26–36, Apr. 2000.
[12] L. Kleinrock, *Queueing Systems, volume I: Theory*: Wiley, 1975.
[13] *Mathematical Handbook*, People's Education Publication House, Beijing, China, 1979.
[14] X. X. Wu, S. H. G. Chan, and B. Mukherjee, "MADF: An novel approach to add an ad hoc overlay on a fixed cellular infrastructure," in *Proc. IEEE WCNC*, vol. 2, Chicago, IL, Sep. 2000, pp. 549–554.
[15] OPNET. MIL 3 Inc.. [Online]. Available: http://www.opnet.com
[16] NOKIA A020 Wireless LAN Access Point. Nokia. [Online]. Available: http://www.nokia.com/corporate/wlan/point_a020.html
[17] D. B. Johnson and D. A. Maltz, "Dynamic source routing in ad hoc wireless networks," in *Mobile Computing*, T. Imielinski and H. Korth, Eds. Boston, MA: Kluwer Academic, 1996, ch. 5, pp. 153–181.
[18] J. Broch, D. B. Johnson, and D. A. Maltz. (1999) The Dynamic Source Routing Protocol for Mobile Ad Hoc Networks. IETF. [Online] draft-ietf-manet-aodv-03.txt
[19] S. M. Jiang, Y. D. Liu, Y. M. Jiang, and Q. H. Yin, "Provisioning of adaptability to variable topologies for routing schemes in MANETs," *IEEE J. Sel. Areas Commun.*, vol. 22, no. 7, pp. 1347–1356, Sep. 2004.

Shengming Jiang (A'96–M'00) received the B.Eng degree from the Shanghai Maritime Institute, China, in 1988, and the DEA and Dr. degrees from the University of Paris VI and the University of Versailles Saint-Quentin-En-Yvelines, France, in 1992 and 1995, respectively.

From 1988 to 1990, he was with Nanjing Petrol Transportation Company, China. He was a Research Associate in the Department of Electrical and Electronic Engineering and the Computer Science Department, The Hong Kong University of Science and Technology, from February 1995 to August 1997. He was a Member of Technical Staff in the Centre for Wireless Communications, National University of Singapore, from September 1997 to July 2000, and a Senior Member of Technical Staff from July 2001 to March 2003. He was an Associate Lead Scientist in the Institute for Infocomm Research, Singapore, from October 2003 to September 2004. Currently, he is a Professor in the School of Electronic and Information Engineering, South China University of Technology. His research interests include networking issues in both wireline and wireless networks.

Dajiang He received the B.Eng. and M.Eng. degrees from Xi'an Jiaotong University, Xi'an, China, in 1995 and 1998, respectively, and the M.Eng. degree from the National University of Singapore in 2001.

In September 2000, he was with MobileOne Asia Pte Ltd. as a System Engineer. Since October 2001, he has been an R&D Engineer in the Institute for Infocomm Research, Singapore, where he works in the Mobile Middleware Lab. Now he is working on the design and implementation of a reliable and robust routing layer for the Sensor Network Flagship Project (SNFP). Previously, he worked on various topics such as routing in mobile ad hoc networks, QoS in IEEE 802.11 and Internet QoS.

Jianqiang Rao received the B.Eng. degree in electrical engineering from Nanchang University, China, in 1994, and the M.Eng. degree in electrical engineering from the National University of Singapore (attached to the Centre for Wireless Communications), Singapore, in 2001.

Currently, he is a 3G Developer with Agere Systems, Munich, Germany, working on delivery of communication solutions for 3G mobile terminals. His research interests include the design of MAC and routing schemes with QoS support in Mobile Ad Hoc Networks.